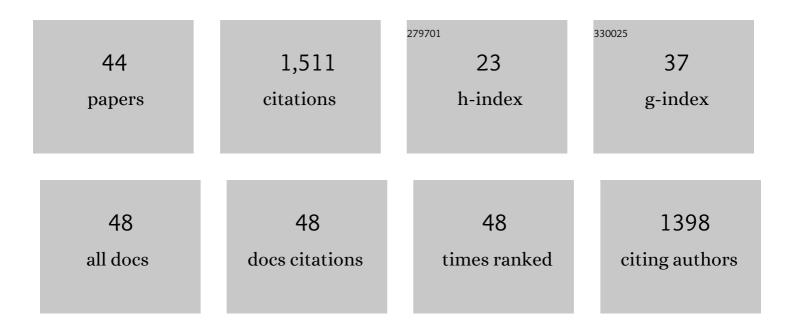
List of Publications by Year in descending order

Source: https://exaly.com/author-pdf/8810715/publications.pdf Version: 2024-02-01



#	Article	IF	CITATIONS
1	Effects of selected functional groups on nanoplastics transport in saturated media under diethylhexyl phthalate co-contamination conditions. Chemosphere, 2022, 286, 131965.	4.2	23
2	Characteristics of cadmium translocation and isotope fractionation in Ricinus communis seedlings: Effects from split/cut-root and limited nutrients. Science of the Total Environment, 2022, 819, 152493.	3.9	3
3	NOM-mineral interaction: Significance for speciation of cations and anions. Science of the Total Environment, 2022, 820, 153259.	3.9	11
4	Aridity influences root versus shoot contributions to steppe grassland soil carbon stock and its stability. Geoderma, 2022, 413, 115744.	2.3	8
5	Effect of Agricultural Organic Inputs on Nanoplastics Transport in Saturated Goethite-Coated Porous Media: Particle Size Selectivity and Role of Dissolved Organic Matter. Environmental Science & Technology, 2022, 56, 3524-3534.	4.6	44
6	Cadmium isotope constraints on heavy metal sources in a riverine system impacted by multiple anthropogenic activities. Science of the Total Environment, 2021, 750, 141233.	3.9	24
7	Watering techniques and zero-valent iron biochar pH effects on As and Cd concentrations in rice rhizosphere soils, tissues and yield. Journal of Environmental Sciences, 2021, 100, 144-157.	3.2	26
8	Source Identification of Heavy Metals in Surface Paddy Soils Using Accumulated Elemental Ratios Coupled with MLR. International Journal of Environmental Research and Public Health, 2021, 18, 2295.	1.2	9
9	Enhanced adsorption of polystyrene nanoplastics (PSNPs) onto oxidized corncob biochar with high pyrolysis temperature. Science of the Total Environment, 2021, 784, 147115.	3.9	56
10	Phosphorus transport in different soil types and the contribution of control factors to phosphorus retardation. Chemosphere, 2021, 276, 130012.	4.2	22
11	Effect of calcium and iron-enriched biochar on arsenic and cadmium accumulation from soil to rice paddy tissues. Science of the Total Environment, 2021, 785, 147163.	3.9	62
12	Comparison of the effects of large-grained and nano-sized biochar, ferrihydrite, and complexes thereof on Cd and As in a contaminated soil–plant system. Chemosphere, 2021, 280, 130731.	4.2	21
13	Competitive adsorption of Dibutyl phthalate (DBP) and Di(2-ethylhexyl) phthalate (DEHP) onto fresh and oxidized corncob biochar. Chemosphere, 2021, 280, 130639.	4.2	20
14	Arsenic and cadmium load in rice tissues cultivated in calcium enriched biochar amended paddy soil. Chemosphere, 2021, 283, 131102.	4.2	18
15	Characterizing Soil Dissolved Organic Matter in Typical Soils from China Using Fluorescence EEM–PARAFAC and UV–Visible Absorption. Aquatic Geochemistry, 2020, 26, 71-88.	1.5	35
16	Hetero-aggregation of goethite and ferrihydrite nanoparticles controlled by goethite nanoparticles with elongated morphology. Science of the Total Environment, 2020, 748, 141536.	3.9	15
17	Redox-dependent effects of phosphate on arsenic speciation in paddy soils. Environmental Pollution, 2020, 264, 114783.	3.7	20
18	Immobilization and release risk of arsenic associated with partitioning and reactivity of iron oxide minerals in paddy soils. Environmental Science and Pollution Research, 2020, 27, 36377-36390.	2.7	5

#	Article	IF	CITATIONS
19	Influence of agricultural organic inputs and their aging on the transport of ferrihydrite nanoparticles: From enhancement to inhibition. Science of the Total Environment, 2020, 719, 137440.	3.9	18
20	Sedimentation and Transport of Different Soil Colloids: Effects of Goethite and Humic Acid. Water (Switzerland), 2020, 12, 980.	1.2	14
21	Enhanced cadmium immobilization in saturated media by gradual stabilization of goethite in the presence of humic acid with increasing pH. Science of the Total Environment, 2019, 648, 358-366.	3.9	42
22	Effects of iron, calcium, and organic matter on phosphorus behavior in fluvo-aquic soil: farmland investigation and aging experiments. Journal of Soils and Sediments, 2019, 19, 3994-4004.	1.5	14
23	Cd, Cu, and Zn Accumulations Caused by Long-Term Fertilization in Greenhouse Soils and Their Potential Risk Assessment. International Journal of Environmental Research and Public Health, 2019, 16, 2805.	1.2	27
24	Fractions and colloidal distribution of arsenic associated with iron oxide minerals in lead-zinc mine-contaminated soils: Comparison of tailings and smelter pollution. Chemosphere, 2019, 227, 614-623.	4.2	41
25	Understanding major NOM properties controlling its interactions with phosphorus and arsenic at goethite-water interface. Water Research, 2019, 157, 372-380.	5.3	48
26	Using chromatographic and spectroscopic parameters to characterize preference and kinetics in the adsorption of humic and fulvic acid to goethite. Science of the Total Environment, 2019, 666, 766-777.	3.9	18
27	Comparisons of heavy metal input inventory in agricultural soils in North and South China: A review. Science of the Total Environment, 2019, 660, 776-786.	3.9	180
28	Influence of calcium and phosphate on pH dependency of arsenite and arsenate adsorption to goethite. Chemosphere, 2018, 199, 617-624.	4.2	67
29	Enhanced transport of ferrihydrite colloid by chain-shaped humic acid colloid in saturated porous media. Science of the Total Environment, 2018, 621, 1581-1590.	3.9	66
30	Remediation of Arsenic contaminated soil using malposed intercropping of Pteris vittata L. and maize. Chemosphere, 2018, 194, 737-744.	4.2	64
31	Distinct effect of humic acid on ferrihydrite colloid-facilitated transport of arsenic in saturated media at different pH. Chemosphere, 2018, 212, 794-801.	4.2	48
32	Migration and transformation of arsenic: Contamination control and remediation in realgar mining areas. Applied Geochemistry, 2017, 77, 44-51.	1.4	48
33	Disparity of Adsorbed Arsenic Species and Fractions on the Soil and Soil Colloids. Procedia Earth and Planetary Science, 2017, 17, 642-645.	0.6	4
34	Micro-distribution of arsenic species in tissues of hyperaccumulator Pteris vittata L Chemosphere, 2017, 166, 389-399.	4.2	16
35	Reduction, methylation, and translocation of arsenic in Panax notoginseng grown under field conditions in arsenic-contaminated soils. Science of the Total Environment, 2016, 550, 893-899.	3.9	30
36	Blocking effect of colloids on arsenate adsorption during co-transport through saturated sand columns. Environmental Pollution, 2016, 213, 638-647.	3.7	50

#	Article	IF	CITATIONS
37	Comparison of chelates for enhancing Ricinus communis L. phytoremediation of Cd and Pb contaminated soil. Ecotoxicology and Environmental Safety, 2016, 133, 57-62.	2.9	69
38	Fractionation of Stable Cadmium Isotopes in the Cadmium Tolerant Ricinus communis and Hyperaccumulator Solanum nigrum. Scientific Reports, 2016, 6, 24309.	1.6	39
39	Stimulation of Fe(II) Oxidation, Biogenic Lepidocrocite Formation, and Arsenic Immobilization by <i>Pseudogulbenkiania</i> Sp. Strain 2002. Environmental Science & Technology, 2016, 50, 6449-6458.	4.6	63
40	An analytical method for precise determination of the cadmium isotopic composition in plant samples using multiple collector inductively coupled plasma mass spectrometry. Analytical Methods, 2015, 7, 2479-2487.	1.3	28
41	Arsenic Adsorption and its Fractions on Aquifer Sediment: Effect of pH, Arsenic Species, and Iron/Manganese Minerals. Water, Air, and Soil Pollution, 2015, 226, 1.	1.1	46
42	Effect of Fluoride on Arsenic Uptake from Arsenic-Contaminated Groundwater usingPteris vittataL International Journal of Phytoremediation, 2015, 17, 355-362.	1.7	8
43	Cadmium accumulation and tolerance of two castor cultivars in relation to antioxidant systems. Journal of Environmental Sciences, 2014, 26, 2048-2055.	3.2	33
44	The Influence Analysis of the Injection Concentration on the Energy Storage in Brackish Aquifers under the Model of Groundwater Flow, Heat Transferring and Solute Movement. , 2011, , .		1